

**Micro Raman characterizations of Pompei's mortars**

Journal:	<i>Journal of Raman Spectroscopy</i>
Manuscript ID:	JRS-07-0137.R1
Wiley - Manuscript type:	Research Article
Date Submitted by the Author:	n/a
Complete List of Authors:	Castriota, Marco; University of Calabria, of Physics Cosco, Valentina; University of Calabria, Physics Barone, Tiziana; University of Calabria, Physics De Santo, Giuseppe; University of Calabria, Physics Carafa, Paolo; University of Calabria, Art History and Archaeology Cazzanelli, Enzo; University of Calabria, Physics
Keywords:	micro-Raman spectroscopy , non-destructive analysis , Mortars, Minerals, Pompei



view

## Micro Raman characterizations of Pompei's mortars

M. Castriota<sup>1\*</sup>, V. Cosco<sup>1</sup>, T. Barone<sup>1</sup>, G. De Santo<sup>1</sup>, P. Carafa<sup>2</sup> and E. Cazzanelli<sup>1</sup>

<sup>1</sup>*INFN-LICRYL Laboratory-CEMIF.CAL, Department of Physics, University of Calabria, Via P.Bucci, Cubo 33B, 87036 Rende (CS) Italy*

<sup>2</sup>*Department of Art History and Archaeology, University of Calabria, Via P.Bucci, 87036 Rende (CS) Italy*

### Abstract.

The ancient town of Pompei offers a unique opportunity to study in details many aspects of the every day life during the Roman early imperial age. The application of micro-Raman spectroscopy can be of great help in performing a reasonably rapid comparative analysis of the mortars, quite useful to ascertain the degree of uniformity of the technical recipes among the various building firms and the eventual technical evolution in the time; moreover, the individuation of minerals of specific geographical origins can give useful information about the extension of commercial intercourses. An example of a micro-Raman investigation on building materials is reported in this work, concerning the analysis of the mortars coming from different points of the wall in the "The House of the Wedding of Hercules". Remarkable differences between ancient and modern mortars are found, allowing a discrimination that can be useful in case of historical building which underwent to several restoration works.

**Keywords:** micro-Raman spectroscopy / non-destructive analysis / Mortars / Minerals / Pompei

\*Corresponding author: M. Castriota, *INFN-LICRYL Laboratory-CEMIF.CAL, Department of Physics, University of Calabria, Via P.Bucci, Cubo 31 C, 87036 Rende (CS) Italy. E-Mail: [Castriota@fis.unical.it](mailto:Castriota@fis.unical.it)*

## INTRODUCTION

In the last years, micro-Raman spectroscopy has been increasingly used as analytical techniques for investigations on historical and cultural artefacts<sup>1</sup>. Its success, first of all, derives from its non-destructive character, but this diagnostic technique results also very specific, sensitive, immune to interference, high spatially refined, and easy to apply, allowing to perform in-situ investigations when optical fiber accessories are employed<sup>2</sup>. It has been applied mainly to pigments detection on many different art objects: i.e. manuscripts, wall paintings, icons, sculpture, paints, papyri, ceramics, pottery and so on<sup>1-16</sup>. Of course it finds application also for the detection of mineral, resin, binding and many (if not all) components of the analysed art object<sup>17-19</sup> and also biomaterials coming from archaeological environments (human and animal tissues, skeletal remains and so on)<sup>20-21</sup>.

Beside the importance for restores and conservators, the knowledge of the material used for realizing the artwork, can allows the historians, for instance, to know whether the artist followed the doctrine of the Academy, or, in contrast, the artist experimented with the most novel pigments available at its time<sup>22-24</sup>.

Generally these studies were focused on a single art object. The present study will explore the chance to use the Raman spectroscopy as a rapid tool to estimate statistically the compositions of different mortars collected from the walls of “*The House of the Wedding of Hercules*” (*Regio VII, insula 9.47*) in the ancient roman city of Pompei. The information on the composition of the mortars can give useful hints about the social organization of the building work in that time. For instance it can ascertain whether the sands used in making the mortars were supplied by a unique sand seller or any small

1  
2  
3  
4 building company provided of that on its own. Answers on such kind of problems will  
5  
6 improve the knowledge of the social and economical life of the people in Pompei town.  
7  
8 Moreover it will be interesting, especially for archaeologists, to explore the possibility  
9  
10 to determine by a non-destructive scientific tool some variation of the sand composition  
11  
12 and relate it with the different period of fabrication of the mortar. In the particular case  
13  
14 of Pompei, archaeologists individuate different construction phases: an older one  
15  
16 starting from sannitic age through the Roman Republic Age and a later phase of  
17  
18 intensive city reconstruction after the earthquake of 62 A.D. and before the Vesuvius  
19  
20 eruption of 79 A.D. In addition there is the important problem to discriminate between  
21  
22 the real ancient roman mortars and those used during the modern restoration works  
23  
24 performed in the last two centuries after the rediscovery of the city, in many cases  
25  
26 without any associated report.  
27  
28  
29  
30  
31

32  
33 Of course, calcium carbonate ( $\text{CaCO}_3$ ) is expected to be the ubiquitous basic component  
34  
35 of all the investigated mortars. It comes by two routes: the well known carbonation  
36  
37 reaction between the  $\text{CO}_2$  and the calcium hydroxide  $\text{Ca}(\text{OH})_2$  and from the marble  
38  
39 powders recycled from the previously destroyed buildings, used to give some “marble  
40  
41 like” translucency to the mortars. The sands, other basic component of the mortars,  
42  
43 came from river ores, because the sea beach sands are not useful for building  
44  
45 applications for their salt content.  
46  
47  
48

49  
50 It is reasonable to think that in the ancient time the sand ores should be very close to  
51  
52 Pompei town. Of course the average compositions of these sands are representative of  
53  
54 the geological composition of the South-West side of the Vesuvius volcano before the  
55  
56 eruption of 79 A.D. Such composition was somewhat different from the present one,  
57  
58 dominated by minerals coming from plinian explosive eruptions, based on acid lava.  
59  
60

1  
2  
3  
4 The ancient geological landscape near Pompei was probably similar to the present one,  
5  
6 on the Northern side near Somma Vesuviana, dominated by alkaline lava coming from  
7  
8 effusive eruptions. All these considerations should provide a frame to classify the  
9  
10 investigated mortars and to help in attributing the age of the fabrication.  
11  
12  
13  
14  
15

## 16 **EXPERIMENTAL**

17  
18  
19  
20  
21 The study has been performed on thirteen specimens of mortars; the first 10 were  
22  
23 collected from different parts of the walls of “*The House of the Wedding of Hercules*”  
24  
25 (Fig. 1), while the last were painted pieces of mortars, collected in the ground inside  
26  
27 the house. Before starting the Raman investigations, these samples have been  
28  
29 catalogued and photographed.  
30  
31  
32

33 The Raman investigation has been performed by using Jobin Yvon micro-Raman  
34  
35 LABRAM instrument, with He-Ne (632.8 nm) laser source using a 50X Olympus  
36  
37 objective with a focal length of 15 mm. The spectral resolution can be estimated at  
38  
39 about  $2\text{ cm}^{-1}$ , with some excess. The illuminated spot size is about  $5\text{ }\mu\text{m}$  of diameter.  
40  
41  
42 Due to the small spot size of the laser many spectra for each sample have been collected  
43  
44 in order to obtain a sampling statistically representative of the materials present on the  
45  
46 samples.  
47  
48  
49

## 50 **RESULTS AND DISCUSSION**

51  
52  
53  
54  
55 Most of the investigated samples shown Raman features typical of different minerals  
56  
57 whose vibrational modes occur in the wavenumber range below  $1150\text{ cm}^{-1}$ . The major  
58  
59 contributes above such wavenumber are coming from carbon inclusions, revealed by the  
60

1  
2  
3  
4 typical D ( $1330\text{ cm}^{-1}$ ) and G ( $1580\text{ cm}^{-1}$ ) bands. For such reason the most representative  
5  
6 Raman spectra collected on the different specimens are shown in figure 2 in the  
7  
8 wavenumber range between  $265$  and  $1150\text{ cm}^{-1}$ . In many cases the resulting Raman  
9  
10 spectra is due to the presence of more substances. However, by selecting many spots on  
11  
12 each sample was possible isolate spectral patterns of specific minerals.  
13  
14

15  
16 The spectrum (a) shows a pattern assigned to minerals of the orthopyroxene group ( $281$ ,  
17  
18  $339$ ,  $385$ ,  $510$ ,  $532$ ,  $665$ ,  $772$ ,  $815$ ,  $825$ ,  $1000$  and  $1038\text{ cm}^{-1}$ )<sup>25,26</sup>. The spectrum (b) is  
19  
20 due to a superposition of materials: the Raman bands at about  $289$ ,  $405$ ,  $493$ ,  $512$  and  
21  
22  $599\text{ cm}^{-1}$  can be assigned to the hematite, while the band at about  $660\text{ cm}^{-1}$  is assigned  
23  
24 to the presence of magnetite<sup>27-32</sup>. These two iron minerals are general associated in the  
25  
26 investigated samples but in some cases the spectrum of isolated magnetite is obtained,  
27  
28 as in spectrum (c). However, some authors assign<sup>33</sup> the band at  $660\text{ cm}^{-1}$  to hematite, as  
29  
30 due to a disorder effect and/or to the presence of nanocrystals of the iron oxide. In the  
31  
32 studied samples it is not possible to discriminate the two cases; since there is evidence  
33  
34 that magnetite (alone) is present (spectrum c), this band will be assigned to magnetite.  
35  
36

37  
38 The spectrum (d), with its Raman features at about  $495$ ,  $526$  and  $958\text{ cm}^{-1}$ , has been  
39  
40 assigned to leucite<sup>34-35</sup>. The spectrum (e) shows a pattern,  $325$ ,  $392$ ,  $495$ ,  $529$ ,  $665$ ,  $1011$   
41  
42 and  $1037\text{ cm}^{-1}$ , due to mixed leucite and pyroxene materials.  
43  
44

45  
46 The spectrum (f) with its modes  $299$ ,  $424$ ,  $600$ ,  $820$ ,  $851$  and  $958\text{ cm}^{-1}$  has been  
47  
48 assigned to forsterite, a mineral of the olivine group, today known as typical of Somma  
49  
50 Vesuviana area, on the northern slopes of the Vesuvius mountain; in addition, like in  
51  
52 many other spectra, low intensity signal at about  $1085\text{ cm}^{-1}$  reveals the presence of  
53  
54 traces of chalk<sup>26,36-37</sup>, because of its binder role.  
55  
56  
57  
58  
59  
60

1  
2  
3  
4 The spectrum (g) is assigned to clinopyroxene with its Raman bands at about 323, 353,  
5  
6 390, 508, 530, 557, 663, 821, 862, 926, 1007 and 1038  $\text{cm}^{-1}$ <sup>25</sup>. Clinopyroxene is still  
7  
8 observed in the spectrum (h), showing a slightly different pattern. The spectrum (i)  
9  
10 shows two broad bands at 484 and 676  $\text{cm}^{-1}$ . The attribution of the broad bands has  
11  
12 been quite difficult, because at first sight they could be due to the presence of  
13  
14 ulvospinel<sup>26</sup>, but the Raman pattern of such mineral shows a different intensity ratio of  
15  
16 those bands. For these reasons the spectrum (i) has been thought due to the contribution  
17  
18 of two substances: the band at 676  $\text{cm}^{-1}$ , has been assigned to the chromite mineral<sup>26,29</sup>  
19  
20 while the band at 484  $\text{cm}^{-1}$  assigned to some mineral of the feldspatoid group such as  
21  
22 analcite<sup>38-40</sup>. The identification of analcite (*analcime*) is also based on the presence in  
23  
24 the spectrum (i) of the bands at 299 and 390  $\text{cm}^{-1}$ , visible in the figure, typical of that  
25  
26 species. The spectrum (j) can be assigned to potassium sodium aluminum silicate like  
27  
28 microcline ( $\text{K}_{1-x}\text{Na}_x\text{AlSi}_3\text{O}_8$ )<sup>40</sup>; nevertheless the contribution of others similar feldspars  
29  
30 cannot be completely excluded. The spectrum (k) shows common features to spectra (b)  
31  
32 and (j), that means that it is due to: hematite, magnetite and microcline. The spectrum (l)  
33  
34 [355, 369, 490, 526, 553, 602, 641, 673, 756, 820, 880, 936 and 983  $\text{cm}^{-1}$ ] can be due to  
35  
36 calcium aluminum silicate like the grossular ( $\text{Ca}_3\text{Al}_2\text{Si}_3\text{O}_{12}$ )<sup>41</sup>. The spectrum (m)  
37  
38 represent the chalk (1085  $\text{cm}^{-1}$ )<sup>30,42</sup>, the spectrum (n) the quartz 466  $\text{cm}^{-1}$ <sup>30,43</sup>, the  
39  
40 spectrum (o) is due to gypsum, with modes at 415, 492 and 1006  $\text{cm}^{-1}$ <sup>30,42-43</sup> associated  
41  
42 to chalk, revealed by the mode at 1086  $\text{cm}^{-1}$ <sup>30,42</sup>. The spectra (p) and (q) 328, 349, 389,  
43  
44 429, 530, 586, 662, 815, 860, 1004, 1047 and 1082  $\text{cm}^{-1}$  are due to clinopyroxene<sup>25</sup>. The  
45  
46 band at about 960 (s) of the spectrum (q) is assigned to apatite<sup>38</sup>. Finally the spectrum  
47  
48 (r) is assigned to a mixture of lead carbonate 1049  $\text{cm}^{-1}$ <sup>42</sup> and quartz 461  $\text{cm}^{-1}$ <sup>30</sup>.  
49  
50  
51  
52  
53  
54  
55  
56  
57  
58  
59  
60

1  
2  
3  
4 In Table 1 are listed the main modes observed on the representatives spectra (see Fig.  
5  
6  
7 2), the substance whose such patterns have been associated and all the samples where  
8  
9 the spectra have been collected. Reorganizing all the experimental findings it has been  
10  
11 possible to list for any sample all the substances observed by micro-Raman  
12  
13 spectroscopy and the results are shown in Table 2. Among all the individuate substances  
14  
15 some are very common while others are very specific. As it was expected, in almost all  
16  
17 the collected spectra the Raman spectrum of chalk ( $\text{CaCO}_3$ ) appears, often as traces of  
18  
19 the binder. In many spots the Raman spectrum of gypsum,  $\text{CaSO}_4 \cdot 2\text{H}_2\text{O}$ , appears,  
20  
21 associated in smaller amount to chalk and in some sample zone, as pure or prevalent  
22  
23 component. In the former case it is possible to explain the sulfate presence as due to  
24  
25 transformations of chalk due to air pollution phenomena, catalyzed in some way by the  
26  
27 action of lichens, bacteria and other microorganisms; even if Pompei is not close to  
28  
29 great industrial areas, degradation phenomena of building and frescoes are however,  
30  
31 well documented<sup>44</sup>. In some case of prevalent gypsum presence, it cannot be excluded  
32  
33 an explanation in terms of wanted addition of such compound to the mortars, in the  
34  
35 modern restoration works.  
36  
37  
38  
39  
40

41  
42 Other minerals very frequently detected in the investigated mortars are hematite and  
43  
44 magnetite, generally associated together, and the minerals of pyroxene group. All these  
45  
46 components are ubiquitously present in the soil of Pompei, and in general, of vesuvian  
47  
48 area, and their presence cannot constitute a discrimination element for the origin of  
49  
50 sands.  
51  
52

53  
54 Others minerals seem to be more specific of single mortar sample or group. This is the  
55  
56 case of forsterite which has been found in S1, S3-S4, S10 samples but never in the  
57  
58 others samples. Forsterite, belonging to the olivine groups, is typically found in the  
59  
60



1  
2  
3  
4 Monte Somma (Somma Vesuvius Complex, Naples province, Campania, Italy) which is  
5  
6 an igneous, arc-shaped mountain representing the remnants of the older volcanic cone  
7  
8 destroyed in the cataclysmic eruption of 79 A.D. <sup>45</sup>, but it was more common in the  
9  
10 ancient geological landscape of all vesuvian area before such eruption. On the basis of  
11  
12 such elements it is reasonable that the sands used for making the ancient mortars  
13  
14 contained a remarkable amount of forsterite; on the contrary the sands used for mortars  
15  
16 in the modern restoration works, in the Pompei area after the eruption, should not  
17  
18 contain an appreciable amount of such mineral. Therefore, that mineral can be proposed  
19  
20 as marker to discriminate between authentic mortars and modern restoration. Taking  
21  
22 into account the mortar samples on the wall of “*The House of the Wedding of*  
23  
24 *Hercules*” it possible to classify as “authentic ancient Roman” the sample S1, S3, S4  
25  
26 and S10, while the others S2, S5-S9, S11-S13 could be assigned to modern mortars.  
27  
28 Such classification match quite well the one derived by archaeological classification of  
29  
30 the parts of the house, that assigns the mortar samples S1-S4 to ancient roman works  
31  
32 and the others S5-S10 to modern restorations. The presence of others minoritarian  
33  
34 components, like grossular, in the mortars classified as “modern”, helps to reinforce this  
35  
36 hypothesis of classification. In conclusion, the resulting evidences obtained by  
37  
38 following two independent routes allow to classify the samples S1, S3 and S4 are  
39  
40 ancient and S5-S9, S11-S13 as modern, while deeper investigations are required for the  
41  
42 samples S2 and S10.  
43  
44  
45  
46  
47  
48  
49  
50  
51  
52  
53

## 54 CONCLUSIONS

55  
56  
57  
58  
59  
60

1  
2  
3  
4 The micro- Raman investigation on several mortars collected mainly from the wall of  
5 the “*House of Hercules weddings*” in Pompei, allows to characterize an average  
6 composition of the sands employed in these mortars. The origin seem always local, but  
7 an appreciable difference in the forsterite content can be associated to the sure ancient  
8 origin of the mortars, against modern restoration works. Presence of calcium sulfate  
9 constitute an evidence of air pollution phenomena.  
10  
11

12 Further investigations and a more detailed statistical analysis are probably useful to  
13 improve the degree of certainty of the statements about the mortars. However, this  
14 experiment to apply micro-Raman analysis to such kind of research seems promising.  
15  
16  
17

### 18 **Acknowledgements**

19 The authors are indebted to Dr. Pier Giovanni Guzzo, Superintendent of Archaeological  
20 Area of Pompei for kindly permitting the collection of the mortars samples and to Dr.  
21 Annamaria Ciarallo for the assistance during these operations. Thanks are due to Prof.  
22 Rosanna De Rosa for providing geological maps of Vesuvius area and Mr. Anselmo  
23 Roberto Calcaterra for helping in the photographic work.  
24  
25

26 This work was partially supported by the *P.O.R 2000-2006 Misura 3.16 e Misura 3.7,*  
27 *Progetto per la realizzazione del Distretto dei Beni Culturali; D.M. 593/2000, Art. 13”:*  
28

29 **LABORATORIO DI SPETTROSCOPIA MICRO-RAMAN PER INDAGINI NON DISTRUTTIVE SU**  
30 **BENI CULTURALI, (LABSRIB).**  
31  
32

### 33 **REFERENCES**

- 34  
35  
36  
37  
38  
39  
40  
41  
42  
43  
44  
45  
46  
47  
48  
49  
50  
51  
52  
53  
54  
55  
56  
57  
58  
59  
60
1. Clark RJH. *Journal of Molecular Structure* 1995; **347**: 417.
  2. Smith GD, Bugio L, Firth S, Clark RJH. *Analytica Chimica Acta* 2001; **440**: 185.

3. Burgio L, Clark RJH, Theodoraki K. *Spectrochimica Acta Part A* 2003; **59**: 2371.
4. Colomban PH. *Appl. Phys. A* 2004; **79**:167.
5. Magistro F, Majolino D, Migliardo P, Ponterio R, Rodriguez Mt. *Journal of Cultural Heritage* 2001; **2**:191.
6. Ruiz-Moreno S, Perez-Pueyo R, Gabaldon A, Soneira MJ, Sandalinas C. *Journal of Cultural Heritage*, 2003; **4**: 309s.
7. Bruni S, Cariati F, Casadio F, Guglielmi V. *Journal of Cultural Heritage* 2001; **4**: 291.
8. Prieto AC, Guedes A, Dória A, Noronha F. *Canadian Journal of Analytical Sciences and Spectroscopy* 2005; **50**: 87.
9. Derbyshire A, Withnall R. *Journal of Raman Spectroscopy* 1999; **30**: 185.
10. Clark RJH, Gibbs PJ. *Journal of Archaeological Science* 1998; **25**: 621.
11. Burgio L, Clark RJH, Gibbs PJ. *Journal of Raman Spectroscopy* 1999; **30**: 181.
12. Vandenberghe P, Lambert K, Matthis S, Schudel W, Bergmans A, Moens L. *Anal. Bioanal. Chem.* 2005; **383**: 707.
13. Bersani D, Antonioli G, Lottici PP, Casoli A. *Spectrochimica Acta Part A* 2003; **59**: 2409.
14. Roascio S, Zucchiatti A, Prati P, Cagnana A. *Journal of Cultural Heritage* 2002; **3**: 289.
15. Bicchieri M, Nardone M, Sodo A. *Journal of Cultural Heritage* 2000; **1**: s277.
16. Burgio L, Melessanaki K, Doulgeridis M, Clark RJH, Anglos D. *Spectrochimica Acta Part B* 2001; **56**: 905.
17. Hope GA, Woods R, Munce CG. *Minerals Engineering* 2001; **14**: 1565.
18. de Faria DLA, Edwards HGM, Afonso MC, Brody RH, Morais JL. *Spectrochimica Acta Part A* 2004; **60**: 1505.
19. Vandenberghe P, Wehling B, Moens L, Edwards H, de Reu M, Van Hooydonk G. *Analytica Chimica Acta* 2000; **407**: 261.
20. Edwards HGM, Munshi T. *Anal. Bioanal Chem.* 2005; **382**: 1398.
21. Wilson AS, Edwards HGM, Farwell DW, Janaway RC. *Journal of Raman Spectroscopy* 1999; **30**: 367.
22. Castro K, Pérez Alonso M, Rodríguez-Laso MD, Madariaga JM. *Spectrochimica Acta Part A* 2004; **60**: 2919.
23. Clark RJH. *Journal of Molecular Structure* 1999; **480-481**: 15.
24. Legodi MA, de Wall D. *Crystal Engineering* 2003; **6**: 287.
25. Mernagh TP, Hoatson DM. *Journal of Raman Spectroscopy* 1997; **28**: 647.
26. Wang A, Kuebler K, Jolliff B, Haskin LA. *Journal of Raman Spectroscopy* 2004; **35**: 504.
27. Zoppi A, Lofrumento C, Castellucci EM, Dejoie C, Sciau Ph. *Journal of Raman Spectroscopy* 2006; **37**: 1131.
28. Bouchard M, Smith DC. *Spectrochimica Acta Part A* 2003; **59**: 2247.
29. Chen M, Xie X, Wang D, Wang S. *Geochimica et Cosmochimica Acta* 2002; **66**: 3143.
30. Smith GD, Clark RJH. *Journal of Archaeological Science* 2004; **31**: 1137.
31. Pérez JM, Esteve-Tébar R. *Archaeometry* 2004; **46**: 607.
32. Perez Leon C, Kador L, zhang M, Muller AHE. *Journal of Raman Spectroscopy* 2004; **35**: 165.

- 1
  - 2
  - 3
  - 4
  - 5
  - 6
  - 7
  - 8
  - 9
  - 10
  - 11
  - 12
  - 13
  - 14
  - 15
  - 16
  - 17
  - 18
  - 19
  - 20
  - 21
  - 22
  - 23
  - 24
  - 25
  - 26
  - 27
  - 28
  - 29
  - 30
  - 31
  - 32
  - 33
  - 34
  - 35
  - 36
  - 37
  - 38
  - 39
  - 40
  - 41
  - 42
  - 43
  - 44
  - 45
  - 46
  - 47
  - 48
  - 49
  - 50
  - 51
  - 52
  - 53
  - 54
  - 55
  - 56
  - 57
  - 58
  - 59
  - 60
33. Bersani D, Lottici PP, Montenero A. *Journal of Raman Spectroscopy* 1999; **30**: 355.
34. Goryainov S. *Phys. Stat. Sol (a): Rapid Research Letter* 2005; **202**: R25.
35. Matson DW, Sharma SK, Philpotts JA. *American Mineralogist* 1986; **71**: 694.
36. Brunetto R, Strazzulla G. *Icarus* 2005; **179**: 265.
37. Bell IM, Clark RJH, Gibbs PJ. *Spectrochimica Acta Part A* 1997; **53**: 2159.
38. [http://www.dst.unisi.it/geofluids/raman/spectrum\\_frame.htm](http://www.dst.unisi.it/geofluids/raman/spectrum_frame.htm)
39. Wang A, Kuebler KE, Jolliff BL, Haskin LA. *American Mineralogist* 2004; **89**: 665.
40. Sharma SK, Lucey PG, Ghosh M, Hubble HW, Horton KA. *Spectrochimica Acta Part A* 2003; **59**: 2391.
41. <http://www.ens-lyon.fr/LST/Raman/index.php>
42. Wehling B, Vandenabeele P, Moens L, Klockenkämper R, von Bohlen A, Van Hooydonk G, de Reu M. *Mikrochim. Acta* 1999; **130**: 253.
43. Darling RS, Ming Chou I, Bodnar RJ. *Science* 1997; **276**: 91.
44. Adam JP. *L'arte di costruire presso i romani, materiali e tecniche*; Ed.VII C.E. Longanesi &Co: Milan, Italy, 2003.
45. <http://www.mindat.org>

Spectra	Main Raman Features (cm <sup>-1</sup> )	Assigned species	Sample
(a)	281(sh), 339(s), 385(sh), 510(m), 532(m), 665(s), 772(sm), 815(m), 825(m), 1000(s), 1038(sm)	Orthopyroxene	S1
(b)	289(s), 405(s), 493(sm), 512(m), 599(s), 660(s),	Hematite & Magnetite	S1, S2, S3, S4, S6, S7, S10, S11, S12
(c)	326(sm,br), 505(sm), 667(s), 996(sm), 1037(vsm),	Magnetite,	S1, S3, S4, S5, S6, S7
(d)	495(s), 526(s), 958(vsm)	Leucite	S1, S7, S12, S13
(e)	325(m), 392(m), 495(m), 529(m), 665(m), 1011(m), 1037(vsm)	Leucite and Pyroxene	S1, S12
(f)	299(sm), 410(sm), 424(sm), 600(m), 820(s), 851(s), 958(m), 1084(sm), 1136(vsm)	Forsterite, Chalk & Gypsum	S1, S3, S4, S10
(g)	323(m), 353(m), 390(m), 508(sm), 530(sm), 557(sm), 663(s), 821(sm), 862(vsm), 926(vsm), 1007(s), 1038(vsm)	Clinopyroxene	S3, S5, S6, S7, S8, S9, S10, S11
(h)	512(vsm), 663(m) 812(m), 825(sm), 964(vsm), 1004(m), 1037(vsm), 1081(vsm)	Clinopyroxene	S1
(i)	299(vsm), 390(sm,br), 484(s), 676(s, br), 1085(vsm)	Chromite & Analcite	S4
(j)	473(s), 514(s), 945(vsm), 1085(vsm)	Microcline (K <sub>1-x</sub> Na <sub>x</sub> )AlSi <sub>3</sub> O <sub>8</sub> Potassium sodium aluminum silicate	S2, S5, S6, S7, S8, S9, S10, S11, S13
(k)	289(m), 405(sm), 476(m), 510(s), 665(s, br), 961(sm)	Hematite, Magnetite & Microcline (K <sub>1-x</sub> Na <sub>x</sub> )AlSi <sub>3</sub> O <sub>8</sub> .	S1, S2, S5, S7
(l)	355(sh), 369(s), 490(vsm), 526(m), 553(vsm), 602(vsm), 641(vsm), 673(vsm), 756(sm, br), 820(sm), 880(m), 936 (vsm), 983 (vsm)	Grossular (Ca <sub>3</sub> Al <sub>2</sub> Si <sub>3</sub> O <sub>12</sub> ) Calcium aluminum silicate	S6
(m)	1085(s)	Calcite	S1, S2, S3, S7, S8, S9, S10, S11, S12, S13
(n)	466(s)	Quartz	S5, S6, S11
(o)	415(vsm), 492(m), 1006(s), 1086(sm)	Chalk & Gypsum,	S2, S6, S9, S10, S11, S13
(p)	327(sm), 355(sm), 391(m), 531(br), 663(s) 1007(m), 1038(vsm), 1082(vsm)	Clinopyroxene	S5, S6, S10
(q)	328(s), 349(sh), 389(m), 429(vsm), 530(sm), 586(vsm), 662(s), 815(m), 860(sm), 960(s), 1004(s), 1047(sm), 1082 (vsm)	Clinopyroxene & apatite	S5, S9
(r)	461(s), 633(vsm), 1049(sm)	Lead carbonate & Quartz .	S2

**Table 1.** Raman Shift and relative intensity of the observed Raman bands and attribution to the relative specie. (vsm) very small, (sm) small, (m) medium, (s) strong, (vs) very strong, (vvs) very very strong, (sh) shoulder, (br) broad, (vbr) very broad.

Sample	Assigned species
S1	Chalk, Clinopyroxene [(Ca,Mg,Fe,Al) <sub>2</sub> (Si,Al) <sub>2</sub> O <sub>6</sub> ], Forsterite [Mg <sub>2</sub> SiO <sub>4</sub> ], Hematite, Leucite [KAlSi <sub>2</sub> O <sub>6</sub> ], Magnetite, Microcline [(K <sub>1-x</sub> Na <sub>x</sub> )AlSi <sub>3</sub> O <sub>8</sub> ], Orthopyroxene [(Mg,Fe,Ca)(Mg,Fe,Al)(Si,Al) <sub>2</sub> O], Pyroxene.
S2	Chalk, Gypsum, Hematite, Lead carbonate, Magnetite, Microcline (K <sub>1-x</sub> Na <sub>x</sub> )AlSi <sub>3</sub> O <sub>8</sub> , Quartz .
S3	Chalk, Clinopyroxene, Forsterite [Mg <sub>2</sub> SiO <sub>4</sub> ], Hematite, Magnetite
S4	Analcite, Chalk, Chromite, Forsterite [Mg <sub>2</sub> SiO <sub>4</sub> ], Hematite, Magnetite
S5	Apatite, Clinopyroxene, Magnetite, Microcline [(K <sub>1-x</sub> Na <sub>x</sub> )AlSi <sub>3</sub> O <sub>8</sub> ], Quartz
S6	Chalk, Clinopyroxene, Gypsum, Grossular [(Ca <sub>3</sub> Al <sub>2</sub> Si <sub>3</sub> O <sub>12</sub> )], Hematite, Magnetite, Microcline [(K <sub>1-x</sub> Na <sub>x</sub> )AlSi <sub>3</sub> O <sub>8</sub> ], Quartz.
S7	Chalk, Clinopyroxene, Hematite, Magnetite, Leucite [KAlSi <sub>2</sub> O <sub>6</sub> ], Microcline [(K <sub>1-x</sub> Na <sub>x</sub> )AlSi <sub>3</sub> O <sub>8</sub> ].
S8	Chalk, Clinopyroxene, Microcline [(K <sub>1-x</sub> Na <sub>x</sub> )AlSi <sub>3</sub> O <sub>8</sub> ]
S9	Apatite, Chalk, Clinopyroxene, Gypsum, Microcline [(K <sub>1-x</sub> Na <sub>x</sub> )AlSi <sub>3</sub> O <sub>8</sub> ]
S10	Chalk, Clinopyroxene, Forsterite [Mg <sub>2</sub> SiO <sub>4</sub> ], Gypsum, Hematite, Magnetite, Microcline [(K <sub>1-x</sub> Na <sub>x</sub> )AlSi <sub>3</sub> O <sub>8</sub> ].
S11	Chalk, Clinopyroxene, Gypsum, Hematite, Magnetite, Microcline [(K <sub>1-x</sub> Na <sub>x</sub> )AlSi <sub>3</sub> O <sub>8</sub> ], Quartz
S12	Chalk, Hematite, Magnetite, Leucite [KAlSi <sub>2</sub> O <sub>6</sub> ] and Pyroxene
S13	Chalk, Gypsum, Leucite [KAlSi <sub>2</sub> O <sub>6</sub> ], Microcline [(K <sub>1-x</sub> Na <sub>x</sub> )AlSi <sub>3</sub> O <sub>8</sub> ]

**Table 2.** Composition of the samples obtained by the Raman investigation.

**Figure captions**

**Figure 1.** Photographs of the “*The House of the Wedding of Hercules*” (*Regio VII, insula 9.47*) in Pompei and of the different analyzed specimens.

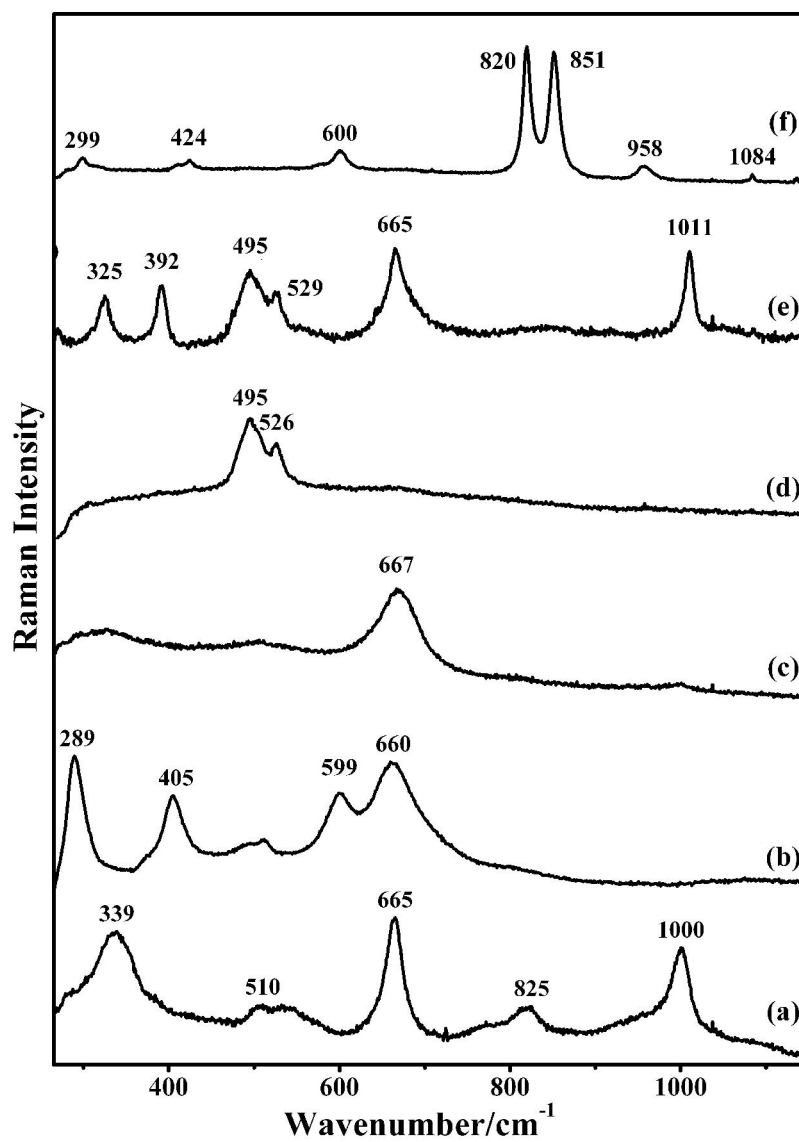
**Figure 2** Representative Raman spectra collected on the different samples. Fig. 2a: spectra (a-f). Fig. 2b: spectra (g-l). Fig. 2c: spectra (m-r). All the spectra are explained in the text.

For Peer Review



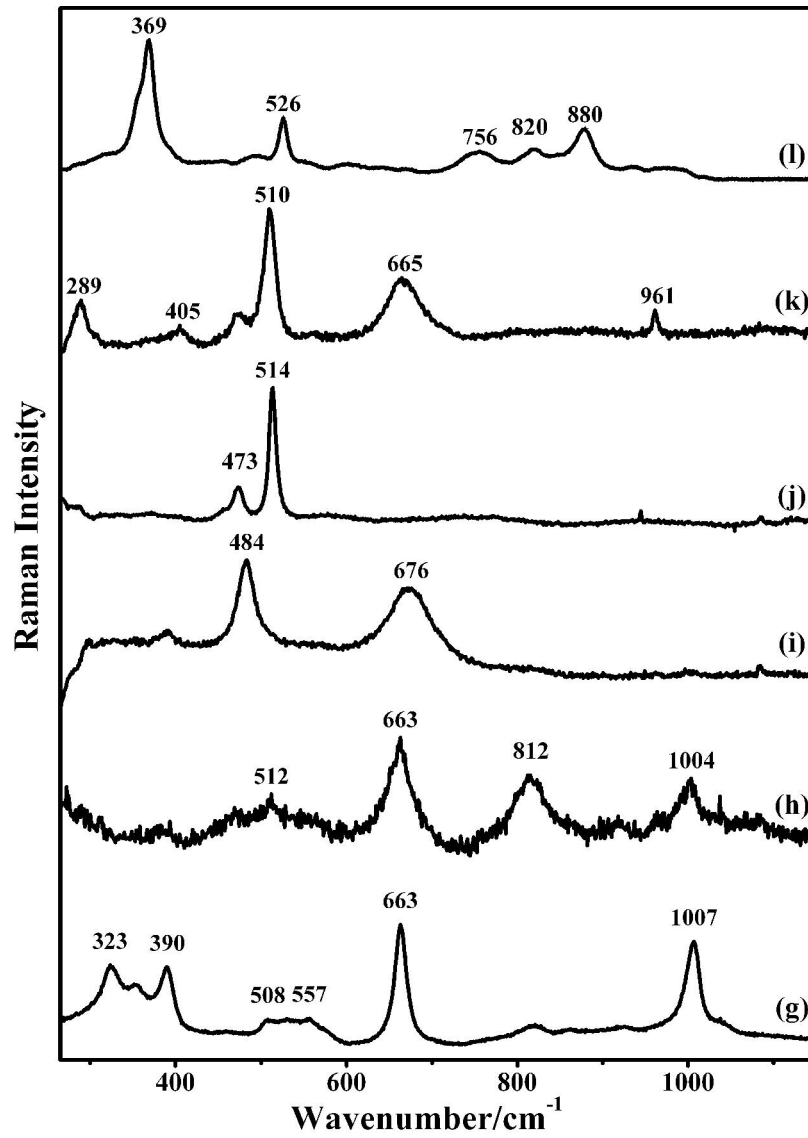


Marco Castriota et al.

**Fig. 2a**

Marco Castriota et al.

Fig. 2b



Marco Castriota et al.

Fig. 2c

